Fully opposite spin polarization of electron and hole bands in DyN and related band structures of GdN and HoN

Tawinan Cheiwchanchamnangij and Walter R. L. Lambrecht

Fully opposite spin-polarization of electron and hole bands in DyN and related band structures of GdN, and HoN

Tawinan Cheiwchanchamnangij[1,2] and Walter R. L. Lambrecht[1]

[1] Department of Physics, Case Western Reserve University, Cleveland, OH 44106-7079 and
[2] Department of Physics, Faculty of Science, Mahidol University, Bangkok 10400, Thailand

Using quasiparticle self-consistent GW calculations, we show that DyN has an unusual nearly zero indirect gap semimetallic band structure in which the states near the valence band maximum are fully minority spin polarized at Γ while the states near the conduction band minimum (at X) have fully majority spin character. This arises due to a strong hybridization of one of the minority spin f-states of Dysprosium with the N-2p bands. The reason why only one of the f bands hybridizes is explained using symmetry arguments. We show that in HoN, this hybridization is already strongly reduced because of the deeper Ho-4f minority spin states.

I. INTRODUCTION

The rare-earth nitrides form an interesting family of materials, sharing the rocksalt structure.[1] Their electronic band structure exhibits varying spin-polarization effects due to the gradually changing localized 4f level occupation. In the past, there has been significant discussion whether they are semimetallic or semiconducting and whether they are ferro- or anti-ferro- magnetic.[2] For a recent discussion and extensive overview of the literature, see Ref. 1. On the experimental side, this uncertainty is related to the difficulty in achieving purely stoichiometric 1:1 RE:N ratio.[3,4] Even small amounts of N-vacancies or oxygen impurities could lead to unintentional n-type doping and hence give the impression of a semimetallic band structure. Likewise, n-type doping may lead to additional carrier-mediated exchange interactions beyond the intrinsic pure material one and obscure the nature of the intrinsic magnetic exchange interactions.[5] On the theory side, the usual underestimate of the gap by the local density approximation or generalized gradient approximation tends to give a semimetallic band structure.[6] The strongly localized 4f electrons exhibit strong correlation effects, which in turn affect the states near the Fermi level. These effects are furthermore sensitive to the lattice constants.[7] Therefore, it is no surprise that the electronic and magnetic properties of these materials continue to be controversial.

Recent experiments[8] on stoichiometric GdN films have identified clearly an optical band gap of about 1.3 eV above the Curie temperature and a 0.4 eV lower gap below the Curie temperature. This agrees well with the theory predictions[6,9] for the direct gap at X but the indirect smaller gap between Γ and X has not yet been observed. The semiconducting nature of the gap of GdN is also consistent with electrical low temperature data.[10] Ferromagnetic ordering is observed experimentally and predicted theoretically by the local spin density functional theory with Hubbard-U corrections (LSDA+U) calculations. To what extent the Curie temperatures from theory and experiment agree is still controversial.[5,7,11] This results from the sensitivity of the exchange interactions to details of the calculations, lattice constant, which density functional or band-structure method is used, and, again, on the possible additional carrier mediated effects. While a lot of the experiment and theory has been focused on the half-filled f shell case of GdN, the situation is less clear for other RE-nitrides.

From the theory point of view, there are two problems to deal with: 1) how to deal with the localized 4f-electrons and 2) how to overcome the gap underestimate of semi-local functionals. The most successful approach today, to deal with the second problem is Hedin's GW approach.[12] In this many-body perturbation theoretical scheme, the self-energy operator $\Sigma(\omega)$, embodying the electron interaction effects on the one-electron states, which then become quasiparticle excitations, is calculated in terms of the one-electron Green's function G and the dynamically screened Coulomb interaction W, which give their name to the approach. While the approach was already proposed in 1965, it took till the late 80s before it became possible to apply it to real materials, first using pseudopotential plane wave methods,[13,14] and eventually all-electron methods.[15,16]

Eventually, it became clear that some form of self-consistency is required to obtain accurate results within an all electron method and the most accurate approach today is the so-called quasiparticle self-consistent GW approach (QSGW)[17,18] in which the starting point independent particle Hamiltonian H^0 includes a non-local but Hermitian exchange-correlation potential derived from the energy dependent $\Sigma = iGW$ in a self-consistent iterative procedure. This method has been shown to give remarkably systematic and accurate results for standard semiconductors and metals.[17]

Its known shortcomings are that the random phase approximation (RPA) used in calculating the screening of the Coulomb interaction $W = \varepsilon^{-1}v = (1 - v\Pi^0)^{-1}v$, with v the bare Coulomb interaction and $\Pi^0 = -iGG$ the irreducible polarization propagator, underestimates the screening because it does not include electron-hole interactions. This tends to underestimate the dielectric

constants by about 20% and hence overestimate the gaps by about 20 %. Unfortunately, it is also known that it tends to overestimate the position of empty f states in RE compounds by several eV, indicating that this underscreening is more severe for such localized states.[9] It does not include multiplet splitting effects for the f-states, which could for example be treated by the Hubbard-I dynamical mean field approach.[19–21] In the present paper, we apply the QSGW approach to a few interesting RE-N keeping in mind the just mentioned short-comings.

The main purpose of the present paper is to point out the possibility of an unusual band structure in DyN. Dysprosium has two additional electrons in the f-band compared to the half-filled GdN case. This leads to two minority spin f-bands crossing through the occupied N-$2p$ bands. We will show below, that one of them leads to an interesting hybridization effect pushing the valence band maximum (VBM) for minority states well above the majority spin ones. Meanwhile the conduction band minimum (CBM) at X shows a significant spin splitting with the majority spin states below the minority spin states. The result is a fully minority spin VBM and fully majority spin CBM. To further study how unique this type of band structure is, we also investigate HoN and discuss TbN based on recent calculations in literature.

II. COMPUTATIONAL METHOD

The full-potential linearized muffin-tin orbital (FP-LMTO) method[22,23] as implemented in the lm-suite[24] is used as band structure method. The band structures are evaluated at the experimental lattice constants. The LSDA+U[25,26] is used as starting point for the QSGW approach,[17,18] available in Ref. 27. It is important to have a starting point with a reasonable description of the $4f$ electronic states, which is not possible in LSDA because it would place the $4f$ electrons at the Fermi-level. The Hubbard-U terms place the occupied (empty) $4f$-derived levels well below (above) the Fermi-level. Within GW theory, however, this splitting should arise from the self-energy Σ. Therefore after the initial LSDA+U calculation of the band structure, which gives the first iteration one-particle Green function G_0 and the corresponding screened Coulomb interaction W_0, the U terms should be switched off. In some cases, it was found that this switching off needs to be done gradually as the iterations progress, so as not to revert back to an unphysical pure LSDA like band structure. The LSDA+U starting point calculation was performed assuming a Hund's rule occupation of the $4f$ levels as starting density matrix.[6]

The details of the QSGW approach as implemented with the FP-LMTO method are given in Kotani et al.[18]. Briefly, a hermitian but non-local exchange correlation potential

$$V_{xc}^{QSGW} = \frac{1}{2} \sum_{ij} |\psi_i\rangle \mathrm{Re}\{\Sigma_{ij}(\epsilon_i) + \Sigma_{ij}(\epsilon_j)\} \langle\psi_j| \quad (1)$$

is derived from the self-energy Σ in the basis set of the one-electron orbitals and iterated to self-consistently. Because off-diagonal elements of Σ are included, it means that the wave functions can become mixed in each iteration and thus wave functions as well as quasiparticle energies are adjusted self-consistently in the procedure. An efficient mixed interstitial plane wave and muffin-tin-orbital product basis set inside the spheres is used.[28] Another important point about this GW implementation is that the atom-centered muffin-tin-orbital basis set allows one to represent the V_{xc}^{QSGW} in real space through an inverse Bloch sum and this allows in turn to obtain an efficient interpolation between **k**-points so that accurate QSGW bands are obtained for any **k**-point in the Brillouin zone. In the present case, a $5 \times 5 \times 5$ **k**-point mesh was used in the GW calculations, while for charge self-consistency a mesh of $10 \times 10 \times 10$ was used. The GW calculations are more sensitive to the basis set used than the LDA calculations. We use a double κ basis set with $l_{max1} = 4$, $l_{max2} = 3$ for Dy. In addition, Dy-$5p$ states and a Dy-$5f$ are added as local orbitals. For N besides the standard double spd basis set, $3s$ and $3p$ states are added as local orbitals. Finally, spd floating orbitals are added in the interstitial region. This highly complete basis set allows for an accurate description of the highly-lying conduction band states. In the calculation of the Σ and Π^0 polarization all bands obtained within the basis set are included in the sums over empty bands. In the present work, we present pure QSGW results. Although this tends to overestimate gaps in standard semiconductors, because of the RPA used in calculating the W or the polarization, we here found it to give already good agreement with experiment for GdN. Finally, we note that spin-orbit coupling can be added to the Hamiltonian at the end but is not carried through in the calculation of the GW self-energy.

III. RESULTS

We start with the band structure of the half-filled case GdN, which has been studied within QSGW before.[9] The band structure is shown in Fig. 1. In this case, spin-orbit coupling is not included because in a half-filled shell, the net orbital moment is zero. We can see that the majority spin $4f$ states lie at about -7.0 to -6.8 eV below the VBM, in fairly good agreement with the X-ray photoelectron spectroscopy (XPS) results of Leuenberger et al.[29] (-7.8 eV) while the minority spin $4f$ bands lie significantly too high at 10 eV as was discussed in Ref. 9. The direct gap at X is 0.859 eV for the majority spins in excellent agreement with experiment[8] for the ferromagnetic state (0.9 eV). The average of up and down spin gap (1.335 eV) also agrees with experiment[8] (1.3 eV) for the paramagnetic state above the Curie temperature. These are pure QSGW results. Therefore, we find no need here to apply a correction for the RPA underscreening. The resulting indirect gap between Γ-X is 0.354 eV. The results

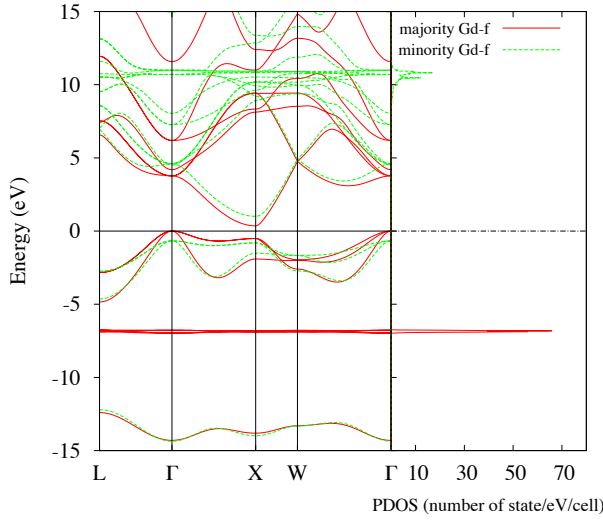FIG. 1: (Color on-line) QSGW band structure of GdN, (red,solid) lines majority spin, (green-dashed) minority spin. Right panel: Gd-4f partial density of states (PDOS).

FIG. 2: (Color on-line) QSGW bands of DyN, (red-solid) line majority spin, (green-dashed) minority spin, Right panel: Dy-4f PDOS.

TABLE I: QSGW band gaps (in eV) compared with experimental results in various RE-N

Compound	Direct $X - X$				Indirect $\Gamma - X$
	maj. $\uparrow$	min. $\downarrow$	av.	expt.	
GdN	0.859	1.811	1.335	1.3 [a]	0.354
DyN	0.683	1.184	0.934	1.5 [b],1.2[c]	−0.454
HoN	1.408	1.671	1.540	1.48 [d]	0.788

[a]From optical absorption, Trodahlet $al.$[8]

[b]From X-ray absorption (XAS) and emission (XES) Preston et $al.$[30]

[c]From optical absorption Azeem et $al.$[31]

[d]From optical absorption Brown et $al.$[32]

are summarized along with other RE-N to be discussed later in Table I.

Next we consider the DyN band structure in Fig. 2. We first discuss the band structure without spin-orbit coupling and later investigate the spin-orbit coupling effects separately. The interesting feature about this band structure is that the VBM near Γ is completely minority-spin-like, while the CBM at X is completely majority-spin-like and dips slightly below the VBM. So, we obtain an indirect semi-metallic band structure between a minority spin VBM and a minority spin CBM. However, the indirect gap between minority spin VBM and minority spin CBM is still 0.101 eV. Dy has two additional occupied minority spin f electrons compared to Gd. We can see that two minority spin f-bands cross through the N-2p bands and one of them has a strong hybridization with the N-2p bands.

This is further shown in Fig.3, in which we highlight the f-character of the bands. We can see that one of the f bands of minority spin runs straight through without any interaction, while the other shows an anti-crossing behavior with the N-2p band. This results in a bond-
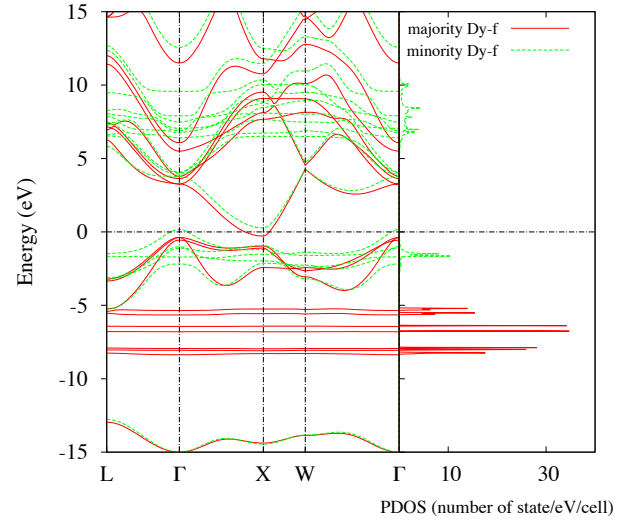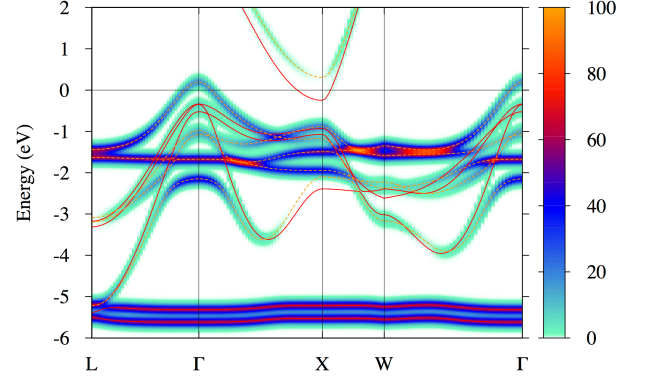

FIG. 3: (Color on-line) Band structure of DyN with color scale representing the 4f contribution of the bands. A "spectral-like function" $A_{RL}(E, \mathbf{k})$ = $\sum_n \delta(E - E_{n\mathbf{k}})|\langle\psi_{n\mathbf{k}}|\phi_{RL}\rangle|^2$ is plotted around each band as a Gaussian with intensity rendered on a color scale. The bands are superposed as red-solid (majority spin) and orange-dashed (minority spin).

ing Dy-4f - N-2p band at Γ at about −2.5 eV, while the corresponding anti-bonding state of minority spin is the VBM. Although this band is then predominantly N-2p like, it still has a substantial Dy-4f contribution. A substantial Dy-4f contribution is also found in the next minority spin band at Γ at about −1.2 eV. At the Brillouin-zone boundaries, L and X, this Dy-4f band almost coincides with the other non-interacting Dy-4f and shows little interaction with the N-2p.

The reason why one 4f band interacts and the other does not at Γ can be explained by symmetry. In the Hund's rule scheme we have added occupied Y_3^3 and Y_3^2 complex spherical harmonic states to maximize $L_z = 5$ and keep L_z parallel to the total $S_z = 5$. The Y_3^3 spheri-

cal harmonics have t_{1u} character in cubic symmetry and are thus allowed to interact with N-p states which share this symmetry. On the other hand, the Y_3^2 spherical harmonic is a mixture of the real $Y_{3,-2} \propto xyz$ state of symmetry a_2 and $Y_{3,2} \propto (x^2 - y^2)z$ of t_{2u} character, neither of which interact with p-states. This explains why only one of the Dy-$4f$ states crossing the N-$2p$ valence band interacts strongly.

Strictly speaking the cubic symmetry is broken by adding a non-zero angular momentum filling of the f states with a net orbital moment. For the majority spin states, this can be seen in the splitting of the N-$2p$ like bands which are no longer three fold degenerate at Γ. This splitting also results from the interaction with the f levels but is much weaker than for minority spin because the majority spin f levels all lie much deeper. However, this symmetry breaking is an artifact of the mean-field treatment in the starting LSDA+U and even in QSGW methods. For a more accurate treatment of the $4f$-states, a dynamic mean field theory including the multiplet splittings of the $4f$-states classified according to their total L and S may be required. This may then also change how f-states of different symmetry interact with the bands. Therefore, it is not clear yet whether the unique band structure found here near the VBM will be upheld in such a more advanced treatment of the $4f$ states.

The CBM at X is similar to that in GdN and has Dy-d_{xy} character for the X point in the [001] direction. This band simply shows the exchange splitting with majority spin below minority spin as expected. The result is a fully opposite spin-polarized character of the band-edges near the gap. This is in some sense an analogue of a half-metal where states at the Fermi level belong to one spin only. It could be advantageous for spintronic applications such as spin-injection or in resonant tunneling type of devices.

The band structure of DyN including spin-orbit coupling is shown in Fig. 4. The spin-orbit coupling Hamiltonian is added here to the Hamiltonian keeping the GW self-energy fixed but the charge density and spin-orbit parameters are allowed to converge to self-consistency. With this approach, we then find indeed a sizable f contribution of $\sim 5\ \mu_B$ to the orbital magnetic moment together with a spin moment of $5\ \mu_B$. The majority spin VBM which was still two-fold degenerate now splits in two with a splitting of about 56 meV. The highest valence band stays dominated by minority spin as can be seen in Fig. 4 which codes the spin-content of the bands in red for minority and blue for majority spin. Similar to the case without spin-orbit coupling, the minority spin VBM lies slightly higher than the majority spin CBM at X. Including the spin-orbit coupling, the indirect gap becomes -0.318 eV. In other words, the Fermi surface would consist of a almost spherical hole pocket of minority spin near Γ and an ellipsoidal electron pocket of majority spin near X. A similar situation of separate electron and hole pockets in the Fermi surface occurs in Fe based chalcogenide and pnictide superconductors,[33,34] although in that case the layered structures lead to cylin-
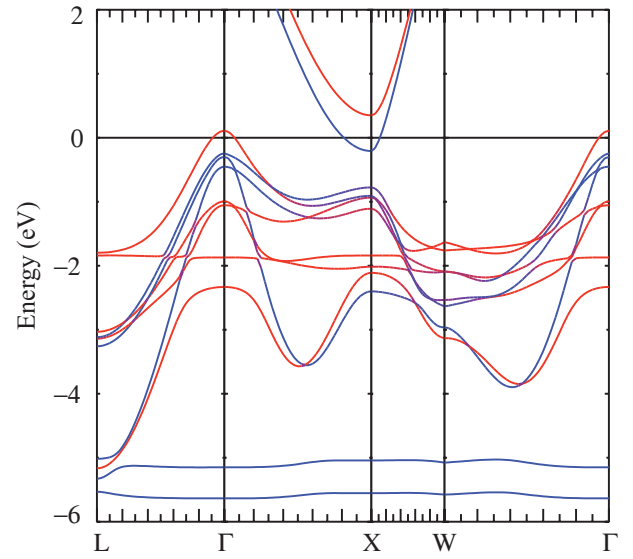

FIG. 4: (Color on-line) Band structure of DyN, including spin-orbit coupling as well as QSGW shift. The spin-content of the bands is coded in red for minority and blue for majority spin. The mixing of the two colors indicates the spin-mixing by spin-orbit coupling.
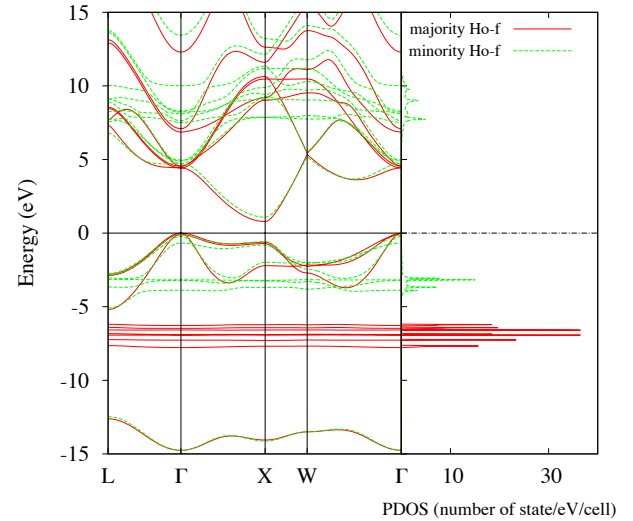

FIG. 5: (Color on-line) QSGW band structure of HoN, red-solid lines majority spin, green-dashed line (minority spin), right panel: Ho-$4f$ PDOS.

drically shaped Fermi surface sheets. The special situation here is that in addition the pockets are completely spin-polarized. The consequences for this in terms of possible pairings in superconductivity remain to be explored.

The band structure of HoN is shown in Fig. 5. It shows that in HoN, the VBM returns to be majority spin-like as in GdN. We can still see some hybridization of one of the minority spin $4f$ bands with N-$2p$ but this now happens deeper in the VBM and the corresponding anti-bonding state at Γ is not sufficiently lifted up to raise above the majority spin VBM. The Ho-$4f$ states already are too

deep to show a significant hybridization with the N-$2p$ bands. Note that the VBM is majority spin-like because of its antibonding interaction with the majority spin-like $4f$ bands below. Although these lie deeper, they apparently have a stronger effect because there are several of them. In this case, we did not include spin-orbit coupling in our discussion because, as we saw in the case of DyN, its overall effects are small. If included, it will of course lead to a net orbital as well as spin magnetic moment as discussed previously in Ref. 6.

One may wonder what would happen in TbN, which corresponds to half-filled +1 f-shell. In a recent study by Peters et al.[21], one can see that both in the cubic and Hund's rule treatment of LSDA+U a minority spin f-band crosses the N-$2p$ bands and it is further concluded by these authors that the cubic symmetry has the lower energy and that in that case the state crossing the VBM has a_2 symmetry. Since the latter cannot interact with p-states, one would not expect a strong hybridization or a minority spin VBM. However, they did not plot band structures, only report densities of states. These authors performed also a DMFT Hubbard-I approximation calculation. In that case the f-multiplet state $^8S_{7/2}$ crosses the N-$2p$ bands fairly close to the VBM. If the cubic symmetry indeed prevails, one would not expect a hybridization of this multiplet state with N-p states. Thus the fully-spin polarized gap states may be quite unique to DyN.

A further word of caution about the present results is required. The occupied $4f$ levels in QSGW may be slightly too shallow. For example, in GdN, we find the $4f$ levels at -7.0 eV, while XPS[29] places them at -7.8 eV. This cannot be explained by the RPA underestimate of W, which would overestimate the binding energy. One may tentatively ascribe it to the vertex Γ in $GW\Gamma$ in the Hedin equations beyond the GW level. Thus, it is possible that including this effect, the $4f$ level in DyN would already shift deeper and reduce the coupling to the VBM of minority spin, which might then no longer cross the majority spin one. At present, to the best of our knowledge no sufficiently detailed experimental knowledge of the spin character of the VBM in DyN is known. Experimental verification would be important either to confirm the unique band structure we proposed here, or if disproven, to provide additional insight in the accuracy of GW for localized $4f$ states.

IV. CONCLUSIONS

We found a unique band structure in DyN, exhibiting a complete opposite spin-polarization of the band edges, with the VBM having minority spin and CBM majority spin character. This was shown to result from a strong hybridization of the minority spin band of t_{1u} symmetry with the N-$2p$ bands at Γ of the same irreducible representation. This leads to an anti-crossing behavior and a significant antibonding Dy-$4f$ character in the VBM of minority spin, sufficiently large to raise it above the majority spin VBM. In HoN, this interaction is already weaker because of the deeper $4f$ level, so that the VBM becomes again majority spin-like as in GdN. Based on analysis of another recent calculation for TbN,[21] we do not expect this unique type of spin-polarized band structure there either. We caution that the result appears to be sensitive to the binding energy of this specific $4f$ state which still requires further testing beyond the GW level and because possibly one needs to include the $4f$ multiplet splittings to obtain the correct symmetry dependent interactions with the N-$2p$ bands. Experimental verification would be strongly desirable, either to exploit the unique opportunities of this new type of spin-polarization of the band gap edge states or to provide deeper insight into the accuracy of GW for f state if the here proposed band structure is invalidated by experiment.

[1] F. Natali, B. Ruck, N. Plank, H. Trodahl, S. Granville, C. Meyer, and W. Lambrecht, Progress in Materials Science **58**, 1316 (2013), ISSN 0079-6425, URL http://www.sciencedirect.com/science/article/pii/S007964251300056X.

[2] C. M. Aerts, P. Strange, M. Horne, W. M. Temmerman, Z. Szotek, and A. Svane, Phys. Rev. B **69**, 045115 (2004), URL http://link.aps.org/doi/10.1103/PhysRevB.69.045115.

[3] D. X. Li, Y. Haga, H. Shida, T. Suzuki, Y. S. Kwon, and G. Kido, Journal of Physics: Condensed Matter **9**, 10777 (1997), URL http://stacks.iop.org/0953-8984/9/i=48/a=019.

[4] P. Wachter, Results in Physics **2**, 90 (2012), ISSN 2211-3797, URL http://www.sciencedirect.com/science/article/pii/S2211379712000174.

[5] A. Sharma and W. Nolting, Phys. Rev. B **81**, 125303 (2010), URL http://link.aps.org/doi/10.1103/PhysRevB.81.125303.

[6] P. Larson, W. R. L. Lambrecht, A. Chantis, and M. van

Schilfgaarde, Phys. Rev. B **75**, 045114 (2007), URL http://link.aps.org/doi/10.1103/PhysRevB.75.045114.

[7] C.-g. Duan, R. F. Sabiryanov, J. Liu, W. N. Mei, P. A. Dowben, and J. R. Hardy, Phys. Rev. Lett. **94**, 237201 (2005), URL http://link.aps.org/doi/10.1103/PhysRevLett.94.237201.

[8] H. J. Trodahl, A. R. H. Preston, J. Zhong, B. J. Ruck, N. M. Strickland, C. Mitra, and W. R. L. Lambrecht, Phys. Rev. B **76**, 085211 (2007), URL http://link.aps.org/doi/10.1103/PhysRevB.76.085211.

[9] A. N. Chantis, M. van Schilfgaarde, and T. Kotani, Phys.Rev. B **76**, 165126 (pages 6) (2007), URL http://link.aps.org/abstract/PRB/v76/e165126.

[10] S. Granville, B. J. Ruck, F. Budde, A. Koo, D. J. Pringle, F. Kuchler, A. R. H. Preston, D. H. Housden, N. Lund, A. Bittar, et al., Phys. Rev. B **73**, 235335 (2006), URL http://link.aps.org/doi/10.1103/PhysRevB.73.235335.

[11] C. Mitra and W. R. L. Lambrecht, Phys. Rev. B **78**, 134421 (2008), URL http://link.aps.org/doi/10.1103/PhysRevB.78.134421.

[12] L. Hedin, Phys. Rev. **139**, A796 (1965).

[13] M. S. Hybertsen and S. G. Louie, Phys. Rev. B **34**, 5390 (1986), URL http://link.aps.org/doi/10.1103/PhysRevB.34.5390.

[14] R. W. Godby, M. Schlüter, and L. J. Sham, Phys. Rev. B **37**, 10159 (1988), URL http://link.aps.org/doi/10.1103/PhysRevB.37.10159.

[15] F. Aryasetiawan and O. Gunnarsson, Reports on Progress in Physics **61**, 237 (1998), URL http://stacks.iop.org/0034-4885/61/i=3/a=002.

[16] W. Ku and A. G. Eguiluz, Phys. Rev. Lett. **89**, 126401 (2002), URL http://link.aps.org/doi/10.1103/PhysRevLett.89.126401.

[17] M. van Schilfgaarde, T. Kotani, and S. Faleev, Phys. Rev. Lett. **96**, 226402 (2006).

[18] T. Kotani, M. van Schilfgaarde, and S. V. Faleev, Phys.Rev. B **76**, 165106 (pages 24) (2007), URL http://link.aps.org/abstract/PRB/v76/e165106.

[19] A. I. Lichtenstein and M. I. Katsnelson, Phys. Rev. B **57**, 6884 (1998), URL http://link.aps.org/doi/10.1103/PhysRevB.57.6884.

[20] J. H. Richter, B. J. Ruck, M. Simpson, F. Natali, N. O. V. Plank, M. Azeem, H. J. Trodahl, A. R. H. Preston, B. Chen, J. McNulty, et al., Phys. Rev. B **84**, 235120 (2011), URL http://link.aps.org/doi/10.1103/PhysRevB.84.235120.

[21] L. Peters, I. Di Marco, P. Thunström, M. I. Katsnelson, A. Kirilyuk, and O. Eriksson, Phys. Rev. B **89**, 205109 (2014), URL http://link.aps.org/doi/10.1103/PhysRevB.89.205109.

[22] M. Methfessel, M. van Schilfgaarde, and R. A. Casali, in *Electronic Structure and Physical Properties of Solids. The Use of the LMTO Method*, edited by H. Dreyssé (Berlin Springer Verlag, 2000), vol. 535 of *Lecture Notes in Physics*, p. 114.

[23] T. Kotani and M. van Schilfgaarde, Phys. Rev. B **81**, 125117 (2010).

[24] http://www.lmsuite.org/.

[25] V. I. Anisimov, J. Zaanen, and O. K. Andersen, Phys. Rev. B **44**, 943 (1991).

[26] A. I. Liechtenstein, V. I. Anisimov, and J. Zaanen, Phys. Rev. B **52**, R5467 (1995).

[27] ecalj package at https://github.com/tkotani/ecalj/. Its one-body part is developed based on Ref.[24].

[28] F. Aryasetiawan and O. Gunnarsson, Phys. Rev. B **49**, 16214 (1994).

[29] F. Leuenberger, A. Parge, W. Felsch, K. Fauth, and M. Hessler, Phys. Rev. B **72**, 014427 (2005), URL http://link.aps.org/doi/10.1103/PhysRevB.72.014427.

[30] A. R. H. Preston, S. Granville, D. H. Housden, B. Ludbrook, B. J. Ruck, H. J. Trodahl, A. Bittar, G. V. M. Williams, J. E. Downes, A. DeMasi, et al., Phys. Rev. B **76**, 245120 (2007), URL http://link.aps.org/doi/10.1103/PhysRevB.76.245120.

[31] M. Azeem, B. J. Ruck, B. D. Le, H. Warring, N. M. Strickland, A. Koo, V. Goian, S. Kamba, and H. J. Trodahl (2012), arXive:1207:6139 [cond-mat].

[32] J. D. Brown, J. E. Downes, C. J. McMahon, B. C. C. Cowie, A. Tadich, L. Thomsen, J. H. Guo, and P. A. Glans, Applied Physics Letters **100**, 072108 (2012), URL http://scitation.aip.org/content/aip/journal/apl/100/7/10.1063/1.3687176.

[33] I. I. Mazin, D. J. Singh, M. D. Johannes, and M. H. Du, Phys. Rev. Lett. **101**, 057003 (2008), URL http://link.aps.org/doi/10.1103/PhysRevLett.101.057003.

[34] D. J. Singh and M.-H. Du, Phys. Rev. Lett. **100**, 237003 (2008), URL http://link.aps.org/doi/10.1103/PhysRevLett.100.237003.